

Boundary element–minimal error method for the Cauchy problem associated with Helmholtz-type equations

Liviu Marin

Received: 23 July 2008 / Accepted: 14 January 2009 / Published online: 7 February 2009
© Springer-Verlag 2009

Abstract An iterative procedure, namely the minimal error method, for solving stably the Cauchy problem associated with Helmholtz-type equations is introduced and investigated in this paper. This method is compared with another two iterative algorithms previously proposed by Marin et al. (Comput Mech 31:367–377, 2003; Eng Anal Bound Elem 28:1025–1034, 2004), i.e. the conjugate gradient and Landweber–Fridman methods, respectively. The inverse problem analysed in this study is regularized by providing an efficient stopping criterion that ceases the iterative process in order to retrieve stable numerical solutions. The numerical implementation of the aforementioned iterative algorithms is realized by employing the boundary element method for both two-dimensional Helmholtz and modified Helmholtz equations.

Keywords Helmholtz-type equations · Inverse problem · Cauchy problem · Regularization · Iterative algorithms · Boundary element method (BEM)

1 Introduction

Helmholtz-type equations characterise many physical applications related to wave propagation and vibration phenomena, as well as heat conduction problems. This class of equations is often used to describe the vibration of a structure [2], the acoustic cavity problem [4], the radiation wave [14], the scattering of a wave [9], the problem of heat conduction in fins [24]. In many engineering problems, either the

boundary conditions are often incomplete, or the geometry of the domain under investigation is not completely known, or the constant, \mathcal{K} , that characterises the Helmholtz-type equation is unknown. These are inverse problems and it is well known that they are generally ill-posed, in the sense that the existence, uniqueness and stability of their solutions are not always guaranteed, see, e.g. Hadamard [8]. A classical example of an inverse boundary value problem associated with Helmholtz-type equations is represented by the Cauchy problem. In this case, boundary conditions are incomplete, in the sense that a part of the boundary of the solution domain is over-specified by prescribing on it both the primary field and its normal derivative, whilst the remaining boundary is under-specified and boundary conditions on the latter boundary have to be determined. The uniqueness of the Cauchy problem is guaranteed without the necessity of removing the eigenvalues for the Laplacian operator, as it happens in the case of direct problems for the Helmholtz equation, see, e.g. Chen and Zhou [3]. However, the Cauchy problem suffers from the non-existence and instability of the solution.

Over the last decades, many theoretical and numerical studies have been devoted to the Cauchy problem associated with Helmholtz-type equations. DeLillo et al. [5] have detected the source of acoustical noise inside the cabin of a midsize aircraft from measurements of the acoustical pressure field inside the cabin by solving a linear Fredholm integral equation of the first kind and they have extended this study to three-dimensional problems, see DeLillo et al. [6]. Marin et al. [31,32] have solved the Cauchy problem associated with the Helmholtz equation using the boundary element method (BEM), in conjunction with an alternating iterative procedure consisting of obtaining successive solutions to well-posed mixed boundary value problems and the conjugate gradient method (CGM), respectively. These iterative methods have been compared with the Tikhonov

L. Marin (✉)
Institute of Solid Mechanics, Romanian Academy,
15 Constantin Mille, Sector 1, P.O. Box 1-863,
010141 Bucharest, Romania
e-mail: marin.liviu@gmail.com

regularization method and singular value decomposition (SVD) by Marin et al. [33], whilst the same authors have proposed an iterative algorithm based on the Landweber–Fridman method (LFM) in combination with the BEM [34]. Jin and Zheng [16] have solved some inverse boundary value problems for the Helmholtz equation using the boundary knot method and a SVD regularization and they have also extended this method to some inverse problems associated with the inhomogeneous Helmholtz equation [17]. The numerical solution for the Cauchy problem for two- and three-dimensional Helmholtz-type equations by employing the method of fundamental solutions (MFS), in conjunction with the Tikhonov regularization method and SVD, has been investigated by Marin and Lesnic [28] and Marin [26], and Jin and Zheng [18], respectively. The Cauchy problem for the Helmholtz equation by employing the Fourier transformation method has been addressed by Tumakov [40], whilst Marin et al. [35] have applied the dual reciprocity BEM (DRBEM), along with the zeroth-order Tikhonov regularization method, to the Cauchy problem for Helmholtz-type equations with variable coefficients. Some spectral regularization methods and a modified Tikhonov regularization method to stabilize the Cauchy problem for the Helmholtz equation at fixed frequency have been proposed by Xiong and Fu [42], whilst Jin and Marin [15] have employed the plane wave method and the SVD to solve stably the same problem. Recently, Wei et al. [41] and Qin et al. [38,39] have reduced the Cauchy problem associated with Helmholtz-type equations to a moment problem and also provided an error estimate and convergence analysis for the latter.

At this stage, it should be mentioned that the non-iterative Tikhonov regularization and truncated SVD methods may produce numerical solutions even when the original Cauchy problem does not have a classical solution, whilst the alternating iterative algorithm described and implemented in Marin et al. [31] is convergent only if the differential operator associated with the governing equation is positive (or negative) definite and self-adjoint. Therefore, for Cauchy problems with disjoint under- and over-specified boundaries the most common methods would be the CGM, LFM and the minimal error method (MEM), see, e.g. King [23]. The main advantage of these methods is that they can be reformulated for L^2 -boundary data, a very desirable feature from the computational point of view. However, in this case the regularity of the solution is affected and this represents an inconvenience of the present method. Furthermore, these three algorithms being iterative methods, it is expected that for exact data they are convergent if and only if the solution of the original Cauchy problem exists. One possible disadvantage of the LFM over the CGM and MEM is represented by the fact that the former is a parameter-dependent method. Consequently, special care should be taken when choosing the parameter associated with the LFM, so that the conver-

gence of this iterative method would be ensured, and this may result in a very large number of iterations performed and hence large computational time.

Motivated by these facts and encouraged by the recent results of Johansson and Lesnic [21] and Marin [27] obtained for the MEM applied to the Cauchy problem associated with the Stokes system in hydrostatics and the Lamé or Navier system in isotropic linear elasticity, respectively, we decided to present and analyse in this paper yet another iterative method for solving the Cauchy problem associated with Helmholtz-type equations, namely the MEM. This iterative method reduces the original Cauchy problem to solving a sequence of two well-posed mixed boundary value problems. It is also numerically proven in this study that, accompanied by a suitable stopping criterion, the MEM has a regularizing/stabilising character. Furthermore, it is shown that this method is very suitable for solving the Cauchy problem in the case of both Helmholtz and modified Helmholtz equations since only a few iterations are required to obtain a stable and accurate numerical solution. Although not presented herein, it is reported that a limitation of the MEM is given by the fact that especially discontinuous Neumann data on the under-specified boundary cannot be accurately recovered by employing the present iterative method. This result is similar to that obtained in the case of isotropic linear elasticity by Marin [27].

The paper is organised as follows: Sect. 2 is devoted to the mathematical formulation of the inverse problem associated with Helmholtz-type equations. The LFM applied to solving the corresponding Cauchy problem, as well as the associated operators, direct and adjoint problems, and convergence theorem, are briefly presented in Sect. 3. Next section, describes the alternatives to the parameter-dependent method described previously, namely the CGM and MEM that are presented in Sects. 4.1 and 4.2, respectively. In Sect. 5, the MEM is applied to solving two Cauchy problems with and without noisy data, for both Helmholtz and modified Helmholtz equations in a two-dimensional doubly connected domain, as described in Sect. 5.1. The MEM is implemented using the BEM, as presented in Sect. 5.2, while at the same time the convergence, stopping regularizing criterion and stability of the method are numerically investigated in Sects. 5.3–5.5, respectively. A comparison of the proposed iterative method with the CGM and LFM, previously analysed by Marin et al. [32,34], respectively, is made in Sect. 5.6. Finally, concluding remarks are provided in Sect. 6.

2 Mathematical formulation

Consider an open bounded domain $\Omega \subset \mathbb{R}^d$, where d is the dimension of the space in which the problem is posed, usually $d \in \{1, 2, 3\}$, and assume that Ω is bounded by a surface

$\Gamma = \partial\Omega$ of class C^2 . We also assume that the boundary consists of two parts, $\Gamma = \Gamma_0 \cup \Gamma_1$, where $\Gamma_0 \neq \emptyset$, $\Gamma_1 \neq \emptyset$ and $\overline{\Gamma_0} \cap \overline{\Gamma_1} = \emptyset$, whilst the primary field T satisfies the Helmholtz-type equation in the domain Ω , namely

$$\mathcal{L}T(\underline{x}) \equiv (\Delta \pm \mathcal{K}^2)T(\underline{x}) = 0, \quad \underline{x} \in \Omega. \tag{1}$$

Here $\Delta = \frac{\partial^2}{\partial x_1^2} + \frac{\partial^2}{\partial x_2^2} + \dots + \frac{\partial^2}{\partial x_d^2}$ is the Laplacian operator, $\mathcal{K} > 0$ and the plus and minus signs correspond to the Helmholtz and modified Helmholtz equations, respectively. We now let $\underline{n}(\underline{x})$ be the outward unit normal at $\underline{x} \in \Gamma$ and $\mathcal{N}T(\underline{x}) \equiv \phi(\underline{x})$ be the normal derivative of the primary field at $\underline{x} \in \Gamma$ defined by

$$\mathcal{N}T(\underline{x}) \equiv \phi(\underline{x}) = \nabla T(\underline{x}) \cdot \underline{n}(\underline{x}), \quad \underline{x} \in \Gamma, \tag{2}$$

where \mathcal{N} is the boundary-differential operator associated with the Helmholtz-type differential operator, \mathcal{L} , and Neumann boundary conditions on Γ .

In the case of the Helmholtz equation, i.e. $\mathcal{L} \equiv \Delta + \mathcal{K}^2$, T is the acoustical field, ϕ is the normal velocity of the sound and $\mathcal{K} > 0$ is the frequency of the acoustical field. If Eq. 1 is regarded as the modified Helmholtz equation, i.e. $\mathcal{L} \equiv \Delta - \mathcal{K}^2$, then T is the dimensionless local fin temperature, ϕ is the dimensionless normal heat flux and $\mathcal{K} = \sqrt{h/(k\delta)}$, where h is the surface heat transfer coefficient, k is the thermal conductivity of the fin and δ is the half-fin thickness, see, e.g. Kraus et al. [24] and Marin et al. [33]. For the sake of the physical explanation, we refer to heat transfer in the following.

In the direct problem formulation, the knowledge of the temperature and/or flux on the whole boundary Γ gives the corresponding Dirichlet, Neumann, or mixed boundary conditions which enables us to determine the temperature distribution in the domain Ω . If it is possible to measure both the temperature and the flux on a part of the boundary Γ , say Γ_0 , then this leads to the mathematical formulation of an inverse problem consisting of Eq. 1 and the boundary conditions

$$T(\underline{x}) = \tilde{T}(\underline{x}), \quad \underline{x} \in \Gamma_0, \tag{3}$$

$$\mathcal{N}T(\underline{x}) \equiv \nabla T(\underline{x}) \cdot \underline{n}(\underline{x}) = \tilde{\phi}(\underline{x}), \quad \underline{x} \in \Gamma_0, \tag{4}$$

where $\tilde{T} \in L^2(\Gamma_0)$ and $\tilde{\phi} \in L^2(\Gamma_0)$ are prescribed functions. In the above formulation of the boundary conditions (3) and (4), it can be seen that the boundary Γ_0 is over-specified by prescribing both the temperature $T|_{\Gamma_0} = \tilde{T}$ and the flux $\phi|_{\Gamma_0} \equiv (\nabla T \cdot \underline{n})|_{\Gamma_0} = \tilde{\phi}$, whilst the boundary Γ_1 is under-specified since both the temperature $T|_{\Gamma_1}$ and the flux $\phi|_{\Gamma_1} \equiv (\nabla T \cdot \underline{n})|_{\Gamma_1}$ are unknown and have to be determined. It should be noted that the problem studied in this paper is of practical importance. For example, the Cauchy problem given by Eqs. 1, 3 and 4, where $\mathcal{L} \equiv \Delta - \mathcal{K}^2$, $\mathcal{K} > 0$, represents the mathematical model for the heat conduction in plate finned-tube heat exchangers, see Kraus et al. [24] and Marin

et al. [33], for which the temperature and the flux can be measured at some points on the fin, whilst both the temperature and the flux are unknown at the fin base or, equivalently, in the tubes.

This problem, termed the Cauchy problem, is much more difficult to solve both analytically and numerically than the direct problem, since the solution does not satisfy the general conditions of well-posedness. In addition, it should be stressed that the Dirichlet, Neumann or mixed direct problems associated to Eq. 1 do not always have a unique solution due to the eigensolutions, see Chen and Zhou [3]. Based on the analytical continuation property, the solution to the Cauchy problem given by Eqs. 1, 3 and 4 is unique if it exists. Moreover, in such cases it is well known that this solution is unstable with respect to small perturbations in the data on Γ_0 , see, e.g. Hadamard [8]. Thus the problem under investigation is ill-posed and we cannot use a direct approach, such as the Gauss elimination method, in order to solve the system of linear equations which arises from the discretisation of the partial differential equations (1) and the boundary conditions (3) and (4). Therefore, knowing either the exact or perturbed data \tilde{T} and $\tilde{\phi}$ on the boundary Γ_0 , in this study we apply and compare three iterative methods, namely the LFM, CGM and MEM, as a consequence of a variational approach to the aforementioned Cauchy problem.

3 A parameter-dependent iterative method

In this section, the operators, direct and adjoint problems, convergence theorem and numerical algorithm corresponding to the Lanweber–Fridman method (LFM) applied to solving the Cauchy problem for Helmholtz-type equations are briefly presented. For more details, we refer the reader to Marin et al. [34] for Helmholtz-type equations, and Johansson [19] and Johansson and Lesnic [22] for the Stokes system in hydrostatics, as well as the complete and rigorous setting of the problem.

3.1 Two direct problems and their associated linear operators

Consider the well-posed, mixed, direct problem for the Helmholtz-type differential operator, \mathcal{L} , with zero Neumann boundary conditions on Γ_0 and non-zero L^2 -Dirichlet boundary conditions on Γ_1 , namely

$$\begin{cases} \mathcal{L}T(\underline{x}) = 0, & \underline{x} \in \Omega, \\ \mathcal{N}T(\underline{x}) = 0, & \underline{x} \in \Gamma_0, \\ T(\underline{x}) = \eta(\underline{x}), & \underline{x} \in \Gamma_1, \end{cases} \tag{5}$$

and the operator associated with this problem (5)

$$\begin{aligned} \mathcal{H} : L^2(\Gamma_1) &\longrightarrow L^2(\Gamma_0), \\ \eta \in L^2(\Gamma_1) &\longrightarrow \mathcal{H}\eta = T|_{\Gamma_0} \in L^2(\Gamma_0). \end{aligned} \tag{6}$$

In a similar manner, consider the well-posed, mixed, direct problem for the Helmholtz-type differential operator, \mathcal{L} , with non-zero L^2 -Neumann boundary conditions on Γ_0 and zero Dirichlet boundary conditions on Γ_1 , i.e.

$$\begin{cases} \mathcal{L}S(\underline{x}) = 0, & \underline{x} \in \Omega, \\ \mathcal{N}S(\underline{x}) = \tilde{\phi}(\underline{x}), & \underline{x} \in \Gamma_0, \\ S(\underline{x}) = 0, & \underline{x} \in \Gamma_1, \end{cases} \tag{7}$$

and its associated operator, namely

$$\begin{aligned} \mathcal{H}_1 : L^2(\Gamma_0) &\longrightarrow L^2(\Gamma_0), \\ \tilde{\phi} \in L^2(\Gamma_0) &\longrightarrow \mathcal{H}_1\tilde{\phi} = S|_{\Gamma_0} \in L^2(\Gamma_0). \end{aligned} \tag{8}$$

It has been shown that the operators \mathcal{H} and \mathcal{H}_1 defined by Eqs. 6 and 8, respectively, are well-defined, linear and bounded and, moreover, the operator \mathcal{H} is also injective and compact, see Marin et al. [34] and Johansson [19]. At this stage, the following remarks should be made:

- (i) Finding a solution $\eta \in L^2(\Gamma_1)$ to the Cauchy problem (1), (3) and (4) is equivalent to finding a solution $\eta \in L^2(\Gamma_1)$ to the following operator equation:

$$\mathcal{H}\eta = \tilde{T} - \mathcal{H}_1\tilde{\phi}. \tag{9}$$

- (ii) If such a solution $\eta \in L^2(\Gamma_1)$ to the Cauchy problem (1), (3) and (4) exists then from definitions (6) and (8) of the operators \mathcal{H} and \mathcal{H}_1 , respectively, it follows that

$$T|_{\Gamma_0} = \tilde{T} - S|_{\Gamma_0}, \tag{10}$$

where T is the solution to the direct problem (5), whilst S solves the direct problem (7).

- (iii) Since \mathcal{H} is a compact operator, it follows that its inverse \mathcal{H}^{-1} is unbounded. Therefore, the operator equation (9) is ill-posed and needs to be regularized.

3.2 Adjoint operator

The Cauchy problem associated with Helmholtz-type equations is regularized by introducing the adjoint operator, \mathcal{H}^* , to the operator \mathcal{H} and the corresponding adjoint problem. The relationship between these two entities is specified in the following:

Lemma 1 [19,34] *Let $\xi \in L^2(\Gamma_0)$. The adjoint operator, \mathcal{H}^* , to the operator \mathcal{H} defined by Eq. 6 is given by*

$$\begin{aligned} \mathcal{H}^* : L^2(\Gamma_0) &\longrightarrow L^2(\Gamma_1), \\ \xi \in L^2(\Gamma_0) &\longrightarrow \mathcal{H}^*\xi = -\mathcal{N}^*S|_{\Gamma_1} \in L^2(\Gamma_1), \end{aligned} \tag{11}$$

where $S \in L^2(\Omega)$ is a solution to the adjoint problem

$$\begin{cases} \mathcal{L}^*S(\underline{x}) = 0, & \underline{x} \in \Omega, \\ \mathcal{N}^*S(\underline{x}) = \xi(\underline{x}), & \underline{x} \in \Gamma_0, \\ S(\underline{x}) = 0, & \underline{x} \in \Gamma_1. \end{cases} \tag{12}$$

It is very important to mention that, in the case of Helmholtz-type equations, $\mathcal{L}^* = \mathcal{L}$ and $\mathcal{N}^* = \mathcal{N}$.

3.3 The Lanweber–Fridman method (LFM)

The following iterative procedure for solving the Cauchy problem associated with Helmholtz-type equations has been proposed, analysed and implemented for the two-dimensional case by Marin et al. [34]:

Step 1. Set $k = 1$ and choose an arbitrary function $\eta^{(k)} \in L^2(\Gamma_1)$.

Step 2. Solve the direct problem

$$\begin{cases} \mathcal{L}T^{(k)}(\underline{x}) = 0, & \underline{x} \in \Omega, \\ \mathcal{N}T^{(k)}(\underline{x}) \equiv \nabla T^{(k)}(\underline{x}) \cdot \underline{n}(\underline{x}) = \tilde{\phi}(\underline{x}), & \underline{x} \in \Gamma_0, \\ T^{(k)}(\underline{x}) = \eta^{(k)}(\underline{x}), & \underline{x} \in \Gamma_1, \end{cases} \tag{13}$$

to determine $T^{(k)}(\underline{x})$, $\underline{x} \in \Omega$, and $\mathcal{N}T^{(k)}(\underline{x}) \equiv \nabla T^{(k)}(\underline{x}) \cdot \underline{n}(\underline{x})$, $\underline{x} \in \Gamma_1$. Set

$$\xi^{(k)}(\underline{x}) = \tilde{T}(\underline{x}) - T^{(k)}(\underline{x}), \quad \underline{x} \in \Gamma_0. \tag{14}$$

Step 3. Solve the adjoint problem

$$\begin{cases} \mathcal{L}^*S^{(k)}(\underline{x}) = 0, & \underline{x} \in \Omega, \\ \mathcal{N}^*S^{(k)}(\underline{x}) \equiv \nabla S^{(k)}(\underline{x}) \cdot \underline{n}(\underline{x}) = \xi^{(k)}(\underline{x}), & \underline{x} \in \Gamma_0, \\ S^{(k)}(\underline{x}) = 0, & \underline{x} \in \Gamma_1, \end{cases} \tag{15}$$

to update the unknown Dirichlet data on Γ_1 as:

$$\eta^{(k+1)}(\underline{x}) = \eta^{(k)}(\underline{x}) - \gamma \mathcal{N}^*S^{(k)}(\underline{x}), \quad \underline{x} \in \Gamma_1, \tag{16}$$

where $0 < \gamma < \|\mathcal{H}\|^{-2}$.

Step 4. Set $k = k + 1$ and repeat Steps 2 and 3 until a prescribed stopping criterion is satisfied.

Finally, we mention the theorem claiming the convergence of the aforementioned iterative algorithm:

Theorem 1 [34] *Let \tilde{T} and $\tilde{\phi}$ be given in $L^2(\Gamma_0)$. Assume that the solution $T \in L^2(\Omega)$ to the Cauchy problem given by Eqs. 1, 3 and 4 exists and choose γ such that $0 < \gamma < \|\mathcal{H}\|^{-2}$. Let $T^{(k)}$ be the k th approximate solution to the algorithm described above. Then*

$$\lim_{k \rightarrow \infty} \|T^{(k)} - T\|_{L^2(\Omega)} = 0, \tag{17}$$

for any initial data $\eta^{(1)} \in L^2(\Gamma_1)$.

It follows from Engl [7] that the procedure presented above is the LFM, see also Landweber [25], is a regularization

method and therefore it works with approximate/noisy data. The LFM has been numerically implemented by Marin et al. [34] for two-dimensional Helmholtz-type equations, Marin and Lesnic [29] in the case of two-dimensional isotropic linear elastic materials, and Johansson and Lesnic [22] for the Stokes system in hydrostatics.

4 Parameter-free iterative methods

From a numerical point of view, it might be difficult to choose an appropriate value for the parameter γ in the right interval $(0, \|\mathcal{H}\|^{-2})$, so that the convergence of the LFM is ensured, see e.g. Theorem 1. In practice, this is achieved by choosing a very small value for the parameter $\gamma > 0$ (usually $\gamma \approx 0.1$) since the norm of the operator \mathcal{H} is very difficult to be estimated. Consequently, as shown in Marin and Lesnic [29], Marin et al. [34] and Johansson and Lesnic [22], in such cases the LFM becomes computationally very slow and in order to overcome this disadvantage, two parameter-free methods are proposed and described in the following.

Consider the operators \mathcal{H} and \mathcal{H}_1 defined by Eqs. 6 and 8, respectively, and denote

$$y \equiv \tilde{T} - \mathcal{H}_1 \tilde{\phi}. \tag{18}$$

Then Eq. 9 becomes

$$\mathcal{H}\eta = y, \tag{19}$$

and the aim is to recover η for a given y .

4.1 The conjugate gradient method (CGM)

The conjugate gradient method (CGM) applied to solving the Cauchy problem for Helmholtz-type equations (1), (3) and (4) is based on the solution of the normal equation associated with Eq. 19, namely

$$\mathcal{H}^* (\mathcal{H}\eta) = \mathcal{H}^* y, \tag{20}$$

and this is equivalent to minimizing the residual functional

$$\mathcal{F}_1 : L^2(\Gamma_1) \longrightarrow [0, \infty), \quad \mathcal{F}_1(\eta) = \|\mathcal{H}\eta - y\|_{L^2(\Gamma_0)}. \tag{21}$$

On using Lemma 1 for the definition of the adjoint operator, \mathcal{H}^* , the following convergent algorithm is obtained, see also Marin et al. [32]:

Step 1. Set $k = 1$ and choose an arbitrary function $\eta^{(k)} \in L^2(\Gamma_1)$.

Step 2. Solve the direct problem

$$\begin{cases} \mathcal{L}T^{(k)}(\underline{x}) = 0, & \underline{x} \in \Omega, \\ \mathcal{N}T^{(k)}(\underline{x}) \equiv \nabla T^{(k)}(\underline{x}) \cdot \underline{n}(\underline{x}) = \tilde{\phi}(\underline{x}), & \underline{x} \in \Gamma_0, \\ T^{(k)}(\underline{x}) = \eta^{(k)}(\underline{x}), & \underline{x} \in \Gamma_1, \end{cases} \tag{22}$$

to determine $T^{(k)}(\underline{x}), \underline{x} \in \Omega$, and $\mathcal{N}T^{(k)}(\underline{x}) \equiv \nabla T^{(k)}(\underline{x}) \cdot \underline{n}(\underline{x}), \underline{x} \in \Gamma_1$. Set

$$\xi^{(k)}(\underline{x}) = \tilde{T}(\underline{x}) - T^{(k)}(\underline{x}), \quad \underline{x} \in \Gamma_0. \tag{23}$$

Step 3. Solve the adjoint problem

$$\begin{cases} \mathcal{L}^* S^{(k)}(\underline{x}) = 0, & \underline{x} \in \Omega, \\ \mathcal{N}^* S^{(k)}(\underline{x}) \equiv \nabla S^{(k)}(\underline{x}) \cdot \underline{n}(\underline{x}) = \xi^{(k)}(\underline{x}), & \underline{x} \in \Gamma_0, \\ S^{(k)}(\underline{x}) = 0, & \underline{x} \in \Gamma_1, \end{cases} \tag{24}$$

to determine

$$\alpha_{k-1} = \begin{cases} 0 & \text{if } k = 1 \\ \|\mathcal{N}^* S^{(k)}\|_{L^2(\Gamma_1)}^2 / \|\mathcal{N}^* S^{(k-1)}\|_{L^2(\Gamma_1)}^2 & \text{if } k > 1 \end{cases} \tag{25}$$

$$\begin{aligned} \zeta^{(k)}(\underline{x}) &= \begin{cases} -\mathcal{N}^* S^{(k)}(\underline{x}), & \underline{x} \in \Gamma_1, \text{ if } k = 1 \\ -\mathcal{N}^* S^{(k)}(\underline{x}) + \alpha_{k-1} \zeta^{(k-1)}(\underline{x}), & \underline{x} \in \Gamma_1, \text{ if } k > 1 \end{cases} \end{aligned} \tag{26}$$

Step 4. Solve the direct problem

$$\begin{cases} \mathcal{L}W^{(k)}(\underline{x}) = 0, & \underline{x} \in \Omega, \\ \mathcal{N}W^{(k)}(\underline{x}) \equiv \nabla W^{(k)}(\underline{x}) \cdot \underline{n}(\underline{x}) = 0, & \underline{x} \in \Gamma_0, \\ W^{(k)}(\underline{x}) = \zeta^{(k)}(\underline{x}), & \underline{x} \in \Gamma_1, \end{cases} \tag{27}$$

to determine

$$\beta_k = \|\mathcal{N}^* S^{(k)}\|_{L^2(\Gamma_1)}^2 / \|W^{(k)}\|_{L^2(\Gamma_0)}^2, \tag{28}$$

$$\eta^{(k+1)}(\underline{x}) = \xi^{(k)}(\underline{x}) + \beta_k \zeta^{(k)}(\underline{x}), \quad \underline{x} \in \Gamma_1. \tag{29}$$

Step 5. Set $k = k + 1$ and repeat Steps 2–4 until a prescribed stopping criterion is satisfied.

It is worth mentioning that the CGM has been implemented for solving numerically the Cauchy problem associated with several partial differential operators, such as the heat equation by Hào and Reinhardt [12] and Bastay et al. [1], the Laplace equation by Hào and Lesnic [13], the Lamé system of linear elasticity by Marin et al. [30], Helmholtz-type equations by Marin et al. [32] and the Stokes system in hydrostatics by Johansson and Lesnic [21].

4.2 The minimal error method (MEM)

The minimal error method (MEM) is a variant of the CGM, see King [23], that minimizes the iteration error functional

$$\mathcal{F}_2 : L^2(\Gamma_1) \longrightarrow [0, \infty), \quad \mathcal{F}_2(\eta) = \|\eta - \mathcal{H}^{-1}y\|_{L^2(\Gamma_1)}, \tag{30}$$

instead of the residual functional \mathcal{F}_1 given by Eq. 21. On using Lemma 1 for the definition of the adjoint operator, \mathcal{H}^* , and the algorithm of Hanke [10] for the Cauchy problem associated with Helmholtz-type equations (1), (3) and (4), the following convergent algorithm is obtained:

Step 1. Set $k = 1$ and choose an arbitrary function $\eta^{(k)} \in L^2(\Gamma_1)$.

Step 2. Solve the direct problem

$$\begin{cases} \mathcal{L}T^{(k)}(\underline{x}) = 0, & \underline{x} \in \Omega, \\ \mathcal{N}T^{(k)}(\underline{x}) \equiv \nabla T^{(k)}(\underline{x}) \cdot \underline{n}(\underline{x}) = \tilde{\phi}(\underline{x}), & \underline{x} \in \Gamma_0, \\ T^{(k)}(\underline{x}) = \eta^{(k)}(\underline{x}), & \underline{x} \in \Gamma_1, \end{cases} \quad (31)$$

to determine $T^{(k)}(\underline{x}), \underline{x} \in \Omega$, and $\mathcal{N}T^{(k)}(\underline{x}) \equiv \nabla T^{(k)}(\underline{x}) \cdot \underline{n}(\underline{x}), \underline{x} \in \Gamma_1$. Set

$$\xi^{(k)}(\underline{x}) = \tilde{T}(\underline{x}) - T^{(k)}(\underline{x}), \quad \underline{x} \in \Gamma_0. \quad (32)$$

Step 3. Solve the adjoint problem

$$\begin{cases} \mathcal{L}^*S^{(k)}(\underline{x}) = 0, & \underline{x} \in \Omega, \\ \mathcal{N}^*S^{(k)}(\underline{x}) \equiv \nabla S^{(k)}(\underline{x}) \cdot \underline{n}(\underline{x}) = \xi^{(k)}(\underline{x}), & \underline{x} \in \Gamma_0, \\ S^{(k)}(\underline{x}) = 0, & \underline{x} \in \Gamma_1, \end{cases} \quad (33)$$

to determine

$$\gamma_{k-1} = \begin{cases} 0 & \text{if } k = 1 \\ \|\xi^{(k)}\|_{L^2(\Gamma_0)}^2 / \|\xi^{(k-1)}\|_{L^2(\Gamma_0)}^2 & \text{if } k > 1 \end{cases} \quad (34)$$

$$\zeta^{(k)}(\underline{x}) = \begin{cases} -\mathcal{N}^*S^{(k)}(\underline{x}), & \underline{x} \in \Gamma_1, \text{ if } k = 1 \\ -\mathcal{N}^*S^{(k)}(\underline{x}) + \gamma_{k-1}\zeta^{(k-1)}(\underline{x}), & \underline{x} \in \Gamma_1, \text{ if } k > 1 \end{cases} \quad (35)$$

$$\delta_k = \|\xi^{(k)}\|_{L^2(\Gamma_0)}^2 / \|\zeta^{(k)}\|_{L^2(\Gamma_1)}^2, \quad (36)$$

$$\eta^{(k+1)}(\underline{x}) = \eta^{(k)}(\underline{x}) + \delta_k \zeta^{(k)}(\underline{x}), \quad \underline{x} \in \Gamma_1. \quad (37)$$

Step 4. Set $k = k + 1$ and repeat Steps 2 and 3 until a prescribed stopping criterion is satisfied.

It should be mentioned that the MEM has recently been implemented for solving numerically the Cauchy problem associated with the Stokes system in hydrostatics and the Lamé or Navier system in isotropic linear elasticity by Johansson and Lesnic [21] and Marin [27], respectively. To our knowledge, the MEM has never been applied to obtaining the numerical solution of the Cauchy problem for Helmholtz-type equations.

5 Numerical results and discussion

In this section, we present the numerical implementation of the MEM using the boundary element method (BEM) in the case of two-dimensional Helmholtz and modified Helmholtz equations and analyse the numerical convergence and stability of this procedure. Furthermore, a comparison of this iterative method with the CGM and LFM previously investigated by Marin et al. [32,34], respectively, is also performed.

5.1 Examples

In order to present and compare the performance of the aforementioned iterative methods, we consider a two-dimensional, smooth, doubly connected geometry, namely the annulus $\Omega = \{\underline{x} = (x_1, x_2) \mid r_{\text{int}}^2 < x_1^2 + x_2^2 < r_{\text{out}}^2\}$, where $r_{\text{int}} = 0.5$ and $r_{\text{out}} = 1.0$, and we solve the Cauchy problem given by Eqs. 1, 3 and 4 for two situations corresponding to both the Helmholtz and modified Helmholtz equations. More precisely, we consider the following analytical solutions for the temperature, T , and normal heat flux, ϕ :

Example I (Two-dimensional modified Helmholtz equation, i.e. $\mathcal{L} \equiv \Delta - \mathcal{K}^2$) We consider the following analytical solution for the temperature:

$$T^{(\text{an})}(\underline{x}) = \exp(a_1x_1 + a_2x_2), \quad \underline{x} = (x_1, x_2) \in \Omega, \quad (38)$$

and the corresponding normal heat flux on the boundary Γ given by:

$$\begin{aligned} \phi^{(\text{an})}(\underline{x}) \equiv \nabla T^{(\text{an})}(\underline{x}) \cdot \underline{n}(\underline{x}) &= [a_1n_1(\underline{x}) + a_2n_2(\underline{x})] \\ &\times T^{(\text{an})}(\underline{x}), \quad \underline{x} = (x_1, x_2) \in \Gamma. \end{aligned} \quad (39)$$

Example II (Two-dimensional Helmholtz equation, i.e. $\mathcal{L} \equiv \Delta + \mathcal{K}^2$) We consider the following analytical solution for the temperature:

$$T^{(\text{an})}(\underline{x}) = \cos(a_1x_1 + a_2x_2), \quad \underline{x} = (x_1, x_2) \in \Omega, \quad (40)$$

and the corresponding normal heat flux on the boundary Γ given by:

$$\begin{aligned} \phi^{(\text{an})}(\underline{x}) \equiv \nabla T^{(\text{an})}(\underline{x}) \cdot \underline{n}(\underline{x}) &= -[a_1n_1(\underline{x}) + a_2n_2(\underline{x})] \\ &\times \sin(a_1x_1 + a_2x_2), \quad \underline{x} = (x_1, x_2) \in \Gamma. \end{aligned} \quad (41)$$

For both examples considered, $\mathcal{K} = 2.0, a_1 = 1.0$ and $a_2 = \sqrt{\mathcal{K}^2 - a_1^2} = \sqrt{3}$. If we denote by $\rho(\underline{x})$ the radial polar coordinate of \underline{x} then the Cauchy problems numerically investigated in this study and associated with the Helmholtz and modified Helmholtz equations corresponding to Examples I and II, respectively, are given by:

Problem I.1 Consider Example I, $\Gamma_0 = \Gamma_{\text{out}} = \{\underline{x} \in \Gamma \mid \rho(\underline{x}) = r_{\text{out}}\}$ and $\Gamma_1 = \Gamma_{\text{int}} = \{\underline{x} \in \Gamma \mid \rho(\underline{x}) = r_{\text{int}}\}$.

Problem I.2 Consider Example I, $\Gamma_0 = \Gamma_{\text{int}} = \{\underline{x} \in \Gamma \mid \rho(\underline{x}) = r_{\text{int}}\}$ and $\Gamma_1 = \Gamma_{\text{out}} = \{\underline{x} \in \Gamma \mid \rho(\underline{x}) = r_{\text{out}}\}$.

Problem II.1 Consider Example II, $\Gamma_0 = \Gamma_{\text{out}} = \{\underline{x} \in \Gamma \mid \rho(\underline{x}) = r_{\text{out}}\}$ and $\Gamma_1 = \Gamma_{\text{int}} = \{\underline{x} \in \Gamma \mid \rho(\underline{x}) = r_{\text{int}}\}$.

Problem II.2 Consider Example II, $\Gamma_0 = \Gamma_{\text{int}} = \{\underline{x} \in \Gamma \mid \rho(\underline{x}) = r_{\text{int}}\}$ and $\Gamma_1 = \Gamma_{\text{out}} = \{\underline{x} \in \Gamma \mid \rho(\underline{x}) = r_{\text{out}}\}$.

5.2 The boundary element method (BEM)

In this section, we briefly describe the BEM for Helmholtz-type equations in two-dimensions, i.e. $d = 2$, although similar arguments apply for higher dimensions, i.e. $d > 2$. The Helmholtz-type equation (1) in the two-dimensional case can be formulated in integral form as, see e.g. Chen and Zhou [3]:

$$c(\underline{x})T(\underline{x}) + \int_{\Gamma} \frac{\partial E(\underline{x}, \underline{y})}{\partial \underline{n}(\underline{y})} T(\underline{y}) d\Gamma(\underline{y}) = \int_{\Gamma} E(\underline{x}, \underline{y})\phi(\underline{y}) d\Gamma(\underline{y}) \tag{42}$$

for $\underline{x} \in \overline{\Omega}$ and $\underline{y} \in \Gamma$, where the first integral is taken in the sense of the Cauchy principal value, $c(\underline{x}) = 1$ for $\underline{x} \in \Omega$ and $c(\underline{x}) = 1/2$ for $\underline{x} \in \Gamma$ (smooth), and E is the real part of the complex fundamental solution for Helmholtz-type equations, which in two-dimensions is given by

$$E(\underline{x}, \underline{y}) = \text{Re} \left\{ \frac{i}{4} H_0^{(1)}(\tilde{k}|\underline{x} - \underline{y}|) \right\}. \tag{43}$$

Here $H_0^{(1)}$ is the Hankel function of order zero of the first kind, $i = \sqrt{-1}$, whilst the constant \tilde{k} is given by $\tilde{k} = \mathcal{K}$ and $\tilde{k} = i\mathcal{K}$ for the Helmholtz and modified Helmholtz equations, respectively. Alternatively, in the case of the two-dimensional modified Helmholtz equation, one can also use its real fundamental solution, whose expression is given by

$$E(\underline{x}, \underline{y}) = \frac{1}{2\pi} K_0(|\underline{x} - \underline{y}|), \tag{44}$$

where K_0 is the modified Bessel function of order zero of the second kind.

A BEM with constant boundary elements, see e.g. Marin et al. [31,32,34], is employed in order to discretise the integral equation (42). If the boundaries Γ_{int} and Γ_{out} are discretised into N_{int} and N_{out} constant boundary elements, respectively, such that $N = N_{\text{int}} + N_{\text{out}}$, then on applying the boundary integral equation (42) at each node/collocation point, we arrive at the following system of linear algebraic equations

$$\mathbf{A} \underline{T} = \mathbf{B} \underline{\phi}. \tag{45}$$

Here \mathbf{A} and \mathbf{B} are matrices which depend solely on the geometry of the boundary Γ and the vectors \underline{T} and $\underline{\phi}$ consist of the discretised values of the boundary temperature and normal heat flux, respectively.

For the inverse problems considered in this study, the BEM system of linear algebraic equations (45) has been solved for each of the well-posed, direct and adjoint problems that occur at each iteration, k , of the LFM, CGM and MEM presented in Sects. 3.3, 4.1 and 4.2, respectively, to provide simultaneously the unspecified boundary temperature and flux on Γ_1 . The number of constant boundary elements used for discretising the boundary Γ was taken to be $N \in \{60, 120, 240\}$

such that $N_{\text{out}} = N_{\text{int}}/2 = N/3$. It is also important to mention that for the Cauchy problems investigated in this paper, as well as all iterative methods analysed herein, the initial guess, $\eta^{(1)}$, for the temperature on the under-specified boundary, Γ_1 , was taken to be

$$\eta^{(1)}(\underline{x}) = 0, \quad \underline{x} \in \Gamma_1. \tag{46}$$

5.3 Convergence of the MEM

In order to investigate the convergence of the algorithm, at every iteration, k , we evaluate the accuracy errors defined by

$$e_T^a(k) = \|T^{(k)} - T^{(\text{an})}\|_{L^2(\Gamma_1)} = \|\eta^{(k)} - T^{(\text{an})}\|_{L^2(\Gamma_1)} \tag{47}$$

and

$$e_{\phi}^a(k) = \|\phi^{(k)} - \phi^{(\text{an})}\|_{L^2(\Gamma_1)} = \|\mathcal{N}T^{(k)} - \phi^{(\text{an})}\|_{L^2(\Gamma_1)} \tag{48}$$

where $T^{(k)}$ and $\phi^{(k)} \equiv \nabla T^{(k)} \cdot \underline{n}$ are the temperature and normal heat flux on the boundary Γ_1 retrieved after k iterations, respectively. The error in predicting the temperature inside the solution domain Ω may also be evaluated by using expression

$$E_T^a(k) = \|T^{(k)} - T^{(\text{an})}\|_{L^2(\Omega)} \tag{49}$$

However, this is not pursued here since the error E_T^a has a similar evolution to that of the errors e_T^a and e_{ϕ}^a , as at each iteration the values of the temperature inside the solution domain Ω are retrieved from the values of the temperature, T , and normal heat flux, ϕ , on Γ .

Figure 1a, b shows, on a logarithmic scale, the accuracy errors e_T^a and e_{ϕ}^a , respectively, as functions of the number of iterations, k , obtained for Problem I.1 with $N \in \{60, 120, 240\}$ when using ‘‘exact’’ boundary data for the inverse problem, i.e. boundary data obtained by solving a direct, well-posed problem, namely

$$\begin{cases} \mathcal{L}T(\underline{x}) = 0, & \underline{x} \in \Omega, \\ T(\underline{x}) = T^{(\text{an})}(\underline{x}), & \underline{x} \in \Gamma_0, \\ \mathcal{N}T(\underline{x}) \equiv \nabla T(\underline{x}) \cdot \underline{n}(\underline{x}) = \phi^{(\text{an})}(\underline{x}), & \underline{x} \in \Gamma_1. \end{cases} \tag{50}$$

It can be seen from these figures that, for all discretisations used in this paper, both errors e_T^a and e_{ϕ}^a keep decreasing until around $k = 75$ iterations, after which the convergence rate of the aforementioned accuracy errors becomes very slow so that they reach a plateau. As expected, for each of the BEM discretisations employed, $e_T^a(k) < e_{\phi}^a(k)$ for all $k > 0$, i.e. temperatures are more accurate than fluxes, and the finer the BEM mesh, the more accurate the numerical results for both the boundary temperature and flux, i.e. the MEM is convergent with respect to refining the mesh size. Furthermore, as N increases, the errors e_T^a and e_{ϕ}^a decrease showing that

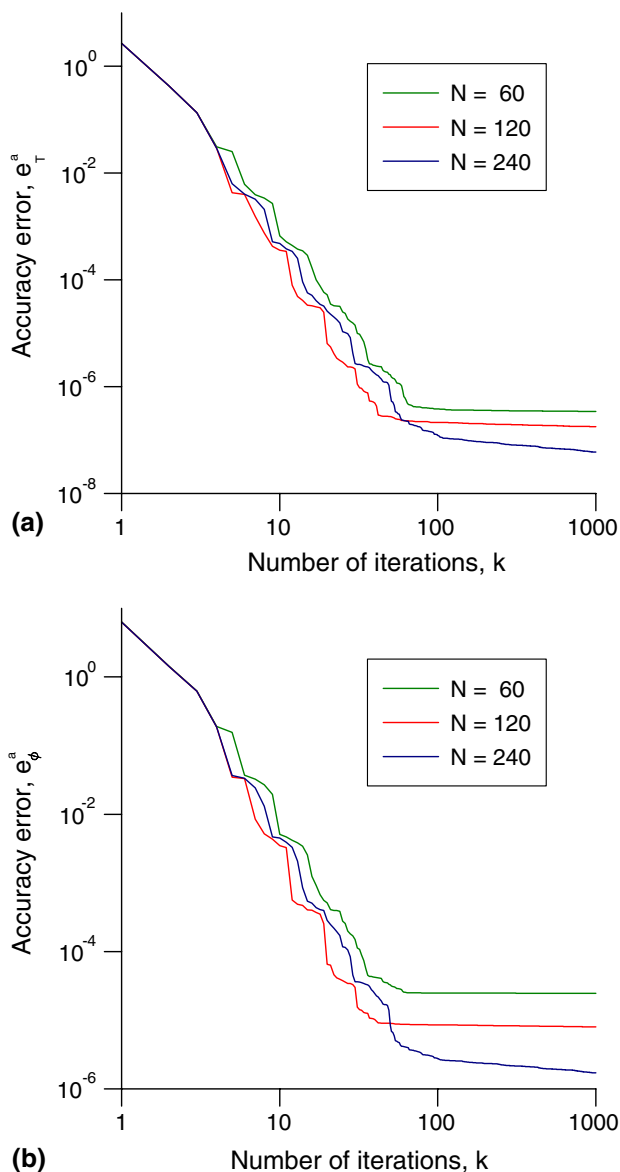


Fig. 1 The accuracy errors (a) e_T^a and (b) e_ϕ^a , as functions of the number of iterations, k , obtained on the under-specified boundary $\Gamma_1 \equiv \Gamma_{\text{int}}$ using the MEM, exact Cauchy data and various numbers of constant boundary elements, namely $N \in \{60, 120, 240\}$, for Problem I.1.

$N \geq 120$ ensures a sufficient discretisation for the accuracy to be achieved.

The same conclusion can be drawn from Fig. 2a, b, which illustrates the analytical and numerical values for the temperature, T , and normal heat flux, ϕ , respectively, obtained on the under-specified boundary Γ_1 for Problem I.1 after $k = 1000$ iterations, for $N \in \{60, 120, 240\}$. From Figs. 1 and 2, it can be concluded that the MEM described in Sect. 4.2 is convergent with respect to increasing the number of iterations, k , as well as refining the BEM mesh size, provided that exact boundary data are prescribed on Γ_0 . Although not presented, it should be mentioned that similar

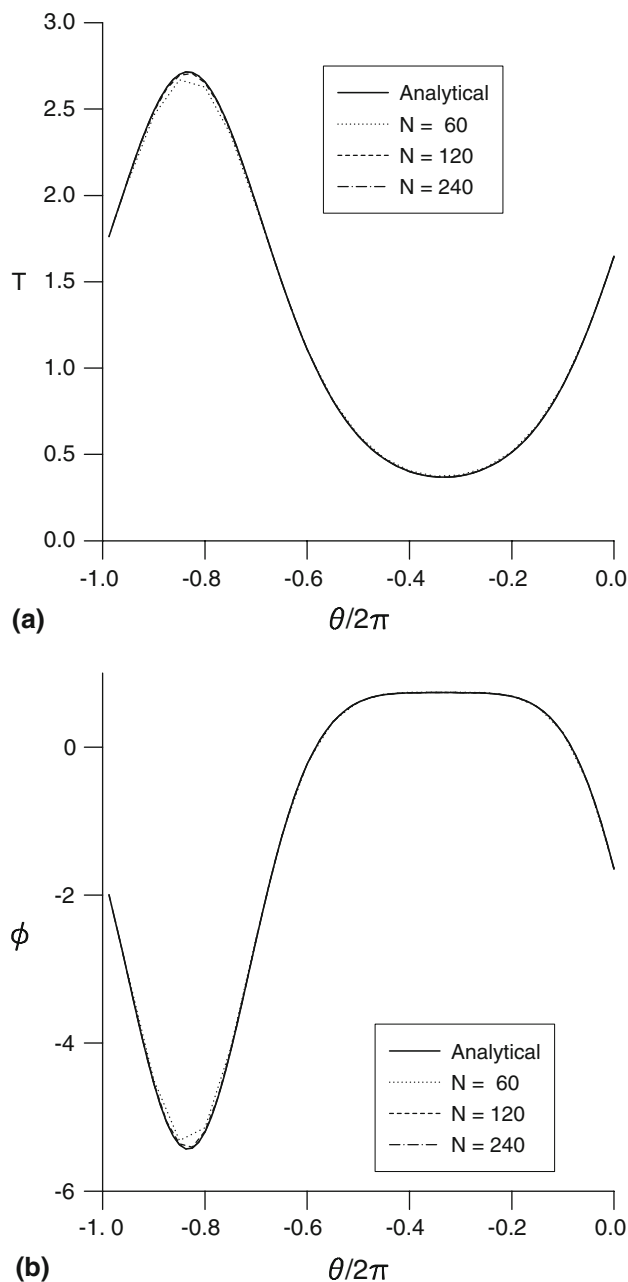


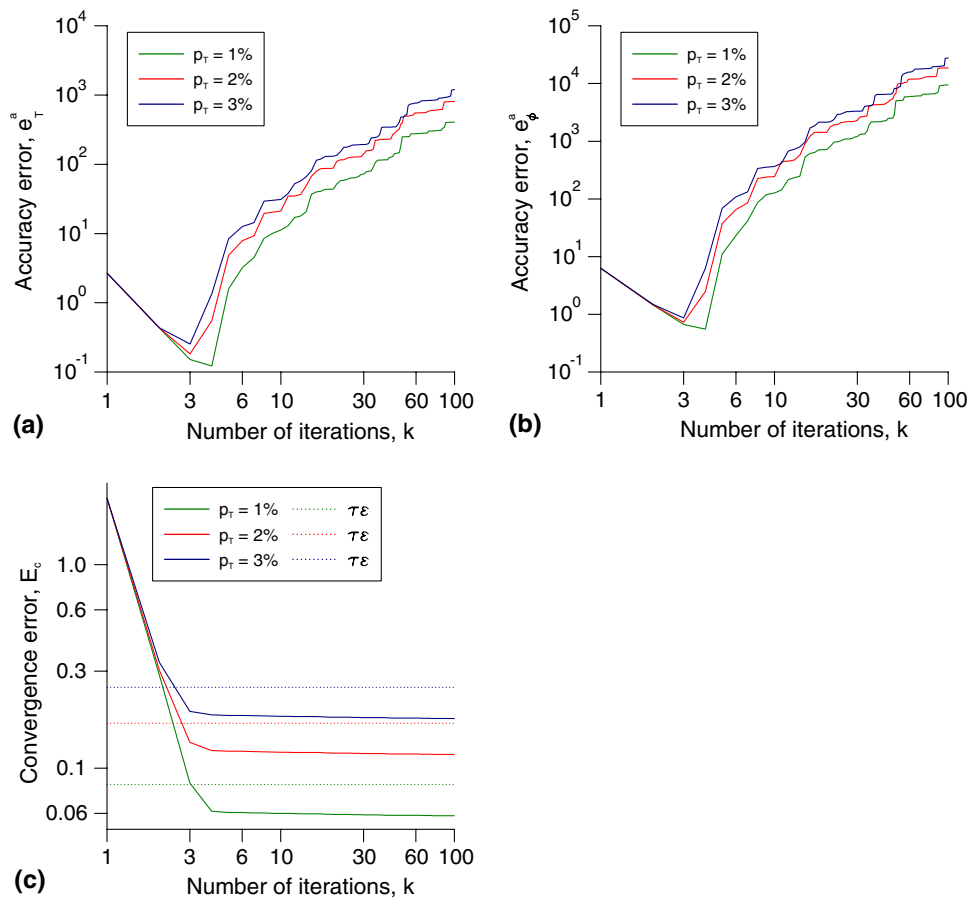
Fig. 2 The analytical (solid line) and numerical (a) temperatures T , and (b) fluxes ϕ , obtained on the under-specified boundary $\Gamma_1 \equiv \Gamma_{\text{int}}$ using the MEM, exact Cauchy data and various numbers of constant boundary elements, namely $N = 60$ (dotted line), $N = 120$ (dashed line) and $N = 240$ (dotted dash line), for Problem I.1.

results have been obtained for the other problems investigated in this study.

5.4 Regularizing stopping criteria

Once the convergence with respect to increasing N of the numerical solution to the exact solution has been established, we fix $N = 240$, i.e. $N_{\text{out}}/2 = N_{\text{int}} = 80$, and investi-

Fig. 3 The accuracy errors (a) e_T^a , and (b) e_ϕ^a , and (c) convergence error, E_c , as functions of the number of iterations, k , obtained using the MEM, the stopping criterion given by Eq. 55 and various relative percentage levels of noise added into the temperature, $T|_{\Gamma_0} \equiv T|_{\Gamma_{out}}$, i.e. $p_T \in \{1\%, 2\%, 3\%\}$, for Problem I.1



gate the stability of the numerical solution for the examples considered. To do so and in order to simulate the inherent inaccuracies in the measured data on Γ_0 , we assume that various relative percentage levels, p_T , of Gaussian random noise have been added into the exact temperature data $T|_{\Gamma_0} = \tilde{T}$, so that the following perturbed temperatures are available:

$$\tilde{T}^\varepsilon \in L^2(\Gamma_0) : \|T^{(an)} - \tilde{T}^\varepsilon\|_{L^2(\Gamma_0)} = \varepsilon. \tag{51}$$

Figure 3a, b presents the accuracy errors e_T^a and e_ϕ^a , respectively, as functions of the number of iterations, k , obtained for $p_T \in \{1, 2, 3\}\%$ in the case of Problem I.1. From these figures it can be seen that as p_T decreases then e_T^a and e_ϕ^a decrease. However, the errors in predicting the temperature and normal heat flux on the under-specified boundary Γ_1 decrease up to a certain iteration number and after that they start increasing. If the iterative process is continued beyond this point then the numerical solutions lose their smoothness and become highly oscillatory and unbounded, i.e. unstable. Therefore, a regularizing stopping criterion must be used in order to terminate the iterative process at the point where the errors in the numerical solutions start increasing.

To define the stopping criteria required for regularizing/stabilizing the iterative methods analysed in this paper, the following two convergence errors are introduced:

$$e_T^c(k) = \|T^{(k)} - \tilde{T}^\varepsilon\|_{L^2(\Gamma_0)} \tag{52}$$

and

$$E_c(k) = \left(\sum_{j=1}^k e_T^c(j)^{-2} \right)^{-1/2}, \tag{53}$$

respectively. In the case of the CGM and LFM, the iterative process is ceased according to the discrepancy principle of Morozov [36], see also Marin et al. [32,34], namely at the optimal iteration number, k_{opt} , given by

$$k_{opt} = \min_{k \in \mathbb{Z}, k > 0} \{e_T^c(k) \leq \tau \varepsilon\}, \tag{54}$$

where $\tau > 1$ is some fixed constant. It is worth mentioning the fact that, according to Nemirovskii [37], the stopping criterion (54) is an order optimal stopping rule for the CGM. Since it was previously shown by Hanke [11] that the discrepancy principle (54) is not a regularizing stopping rule for the MEM, then based on the convergence error, E_c , given by

Eq. 53, the iterative process is ceased in this case at the following optimal iteration number:

$$k_{\text{opt}} = \min_{k \in \mathbb{Z}, k > 0} \{E_c(k) \leq \tau \varepsilon\}, \quad (55)$$

where $\tau > 1$ is some fixed constant.

Figure 3c presents the evolution of the convergence error E_c with respect to the number of iterations performed, k , using various relative percentage levels of Gaussian noise added into the temperature on the over-specified boundary Γ_0 , namely $p_T \in \{1\%, 2\%, 3\%\}$, and $\tau \approx 1.35$ in the stopping criterion (55), for Problem I.1. By comparing Fig. 3a–c, it can be seen that selecting the optimal iteration number, k_{opt} , according to the stopping rule given by Eq. 55 captures very well the minimum values for the accuracy errors e_T^a and e_ϕ^a ; therefore, Eq. 55 represents a stabilizing stopping criterion for the MEM. Although not illustrated, it is important to mention that similar results and conclusions have been obtained for the other Cauchy problems investigated in this paper.

As mentioned in the previous section, for exact data the iterative process is convergent with respect to increasing the number of iterations, k , since the accuracy errors e_T^a and e_ϕ^a keep decreasing even after a large number of iterations, see Fig. 1a, b. It should be noted that a stopping criterion is not necessary in this case since the numerical solution is convergent with respect to increasing the number of iterations. However, even in this situation E_c , e_T^a and e_ϕ^a have a similar behaviour and the error E_c may be used to stop the iterative process at the point where the rate of convergence is very small and no substantial improvement in the numerical solution is obtained even if the iterative process is continued. Therefore, it can be concluded that the regularizing stopping criterion proposed for the MEM is very efficient in locating the point where the errors start increasing and the iterative process should be ceased.

5.5 Stability of the MEM

Although for the LFM and CGM the choice of τ close to unity results in accurate and stable results for the temperature and flux on the under-specified boundary Γ_1 , in the case of the MEM values for τ between 1.0 and 1.1 produce numerical results exhibiting a slightly oscillatory unstable behaviour for the aforementioned temperature and flux. Consequently, this study shows that the MEM is more sensitive to the choice of τ than in the other iterative methods, as something expected from the preliminary investigation of King [23] and also in accordance with the recent results of Johansson and Lesnic [20] and Marin [27]. Also, it should be mentioned that a value of $\tau \approx 1.35$ was found to be optimal for the MEM for all levels of noise, as well as all inverse prob-

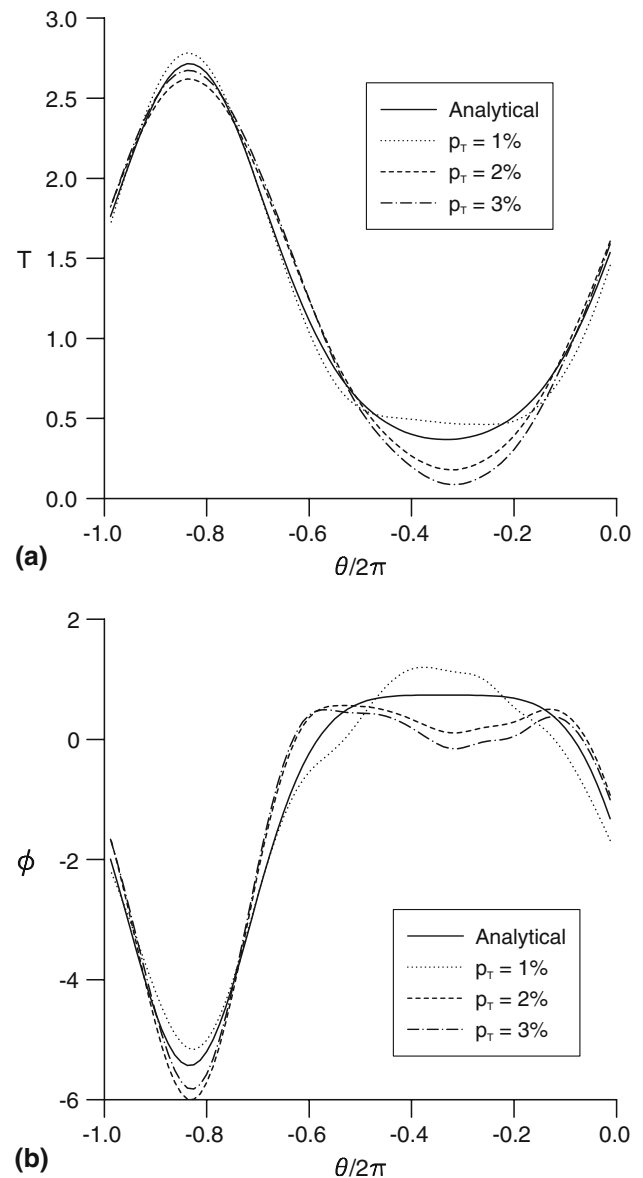
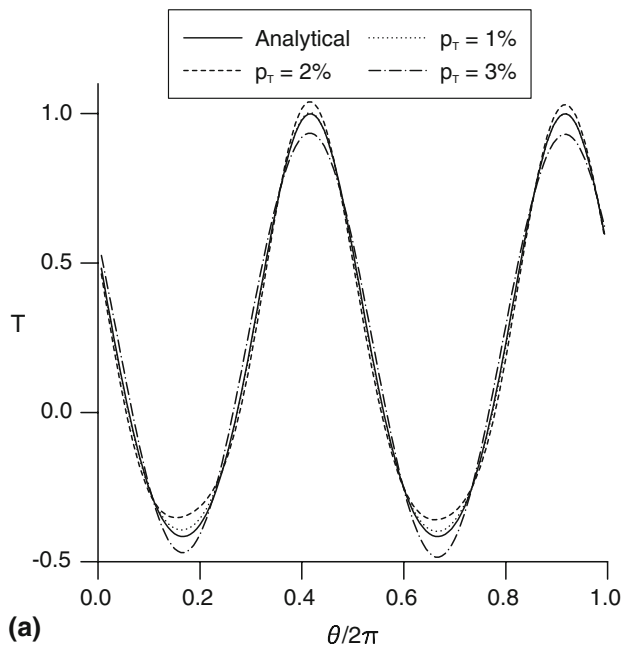


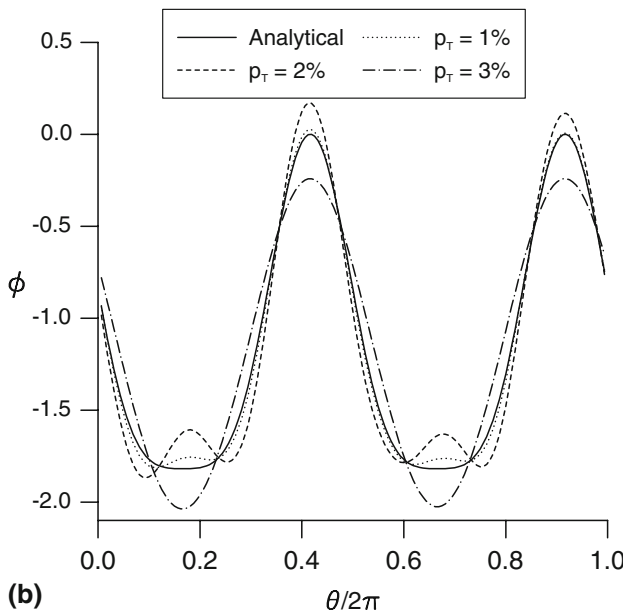
Fig. 4 The analytical (solid line) and numerical (a) temperatures T , and (b) fluxes ϕ , obtained on the under-specified boundary $\Gamma_1 \equiv \Gamma_{\text{int}}$ using the MEM, the stopping criterion given by Eq. 55 and various relative percentage levels of noise added into the temperature, $T|_{\Gamma_0} \equiv T|_{\Gamma_{\text{out}}}$, i.e. $p_T = 1\%$ (dotted line), $p_T = 2\%$ (dashed line) and $p_T = 3\%$ (dotted dash line), for Problem I.1

lems investigated in this paper, as reported by Johansson and Lesnic [20] and Marin [27] for the Stokes system in hydrostatics and the Lamé or Navier system in isotropic linear elasticity, respectively.

Based on the stopping criterion (55) described in Sect. 5.4, the numerical results obtained for the temperature obtained on the under-specified boundary $\Gamma_1 \equiv \Gamma_{\text{int}}$ and its corresponding analytical value are presented in Fig. 4a, for various amounts of noise added into the temperature, $T|_{\Gamma_0} \equiv T|_{\Gamma_{\text{out}}}$, i.e. $p_T \in \{1\%, 2\%, 3\%\}$, in the case of Problem I.1. The



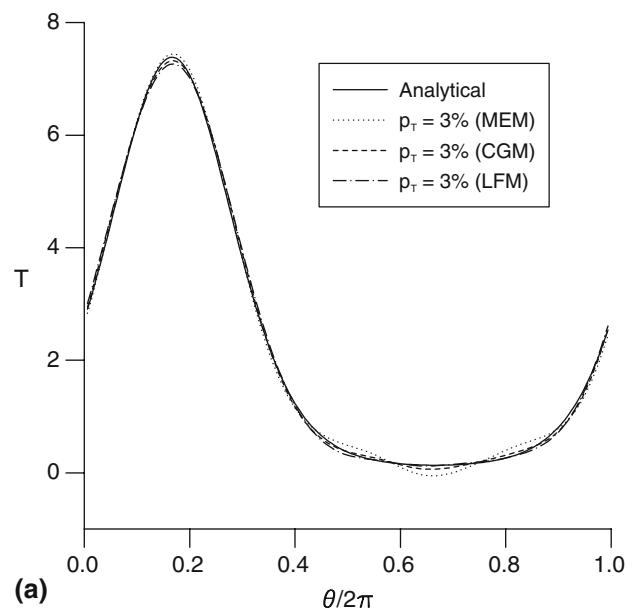
(a)



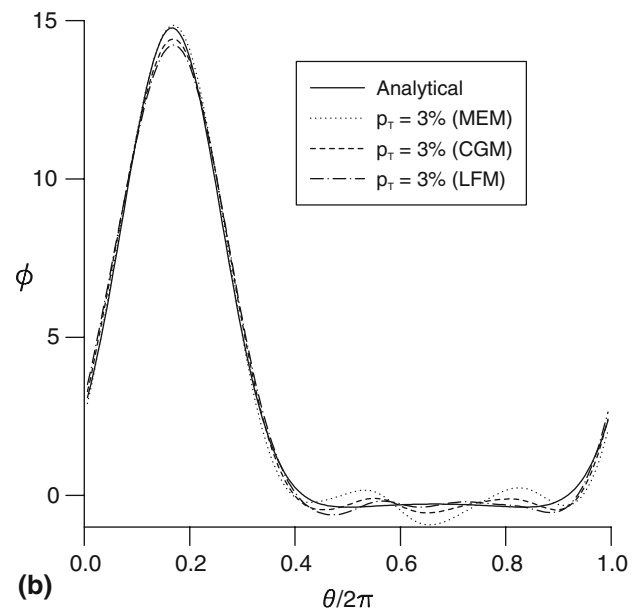
(b)

Fig. 5 The analytical (solid line) and numerical (a) temperatures T , and (b) fluxes ϕ , obtained on the under-specified boundary $\Gamma_1 \equiv \Gamma_{out}$ using the MEM, the stopping criterion given by Eq. 55 and various relative percentage levels of noise added into the temperature, $T|_{\Gamma_0} \equiv T|_{\Gamma_{int}}$, i.e. $p_T = 1\%$ (dotted line), $p_T = 2\%$ (dashed line) and $p_T = 3\%$ (dotted dash line), for Problem II.2

associated analytical and numerical values for the normal heat flux ϕ , retrieved on Γ_1 using the MEM and the stopping criterion (55), are illustrated in Fig. 4b. From these figures it can be seen that the numerical solution, for both the temperature and normal heat flux, is a stable approximation to the corresponding exact solution, free of unbounded and rapid oscillations, and it converges to the exact solution as the



(a)



(b)

Fig. 6 The analytical (solid line) and numerical (a) temperatures T , and (b) fluxes ϕ , obtained on the under-specified boundary $\Gamma_1 \equiv \Gamma_{out}$ using $N_{out} = 160$ and $N_{int} = 80$ constant boundary elements for discretising Γ_{out} and Γ_{int} , respectively, the MEM (dotted line), CGM (dashed line) and LFM (dotted dash line), and $p_T = 3\%$ relative percentage noise added into the boundary temperature, $T|_{\Gamma_0} \equiv T|_{\Gamma_{int}}$, for Problem I.2

relative percentage level of noise, p_T , added into the input boundary data decreases.

The same conclusion can be drawn from Fig. 5a, b which presents the numerical values for the temperature and normal heat flux, in comparison with their analytical counterparts, obtained on the under-specified boundary $\Gamma_1 \equiv \Gamma_{out}$ using the MEM, the regularizing stopping criterion (55) and

Table 1 The values of the optimal iteration number, k_{opt} , the corresponding accuracy errors, $e_T^a(k_{\text{opt}})$ and $e_\phi^a(k_{\text{opt}})$, the convergence error, $e_T^c(k_{\text{opt}})$ or $E_c(k_{\text{opt}})$, and the computational time, obtained using $N_{\text{out}} = 160$ and $N_{\text{int}} = 80$ constant boundary elements for

discretising the outer and inner boundaries, respectively, the CGM, LFM and MEM and various relative percentage levels of noise added into the boundary temperature data, i.e. $p_T \in \{1\%, 2\%, 3\%\}$, for Problem I.2.

Method	p_T (%)	$e_T^a(k_{\text{opt}})$	$e_\phi^a(k_{\text{opt}})$	$e_T^c(k_{\text{opt}})/E_c(k_{\text{opt}})$	k_{opt}	CPU time (s)
CGM	1	0.45987×10^{-1}	0.21079×10^0	0.14127×10^{-1}	7	66.03
	2	0.12937×10^0	0.56175×10^0	0.28510×10^{-1}	5	64.73
	3	0.13870×10^0	0.58972×10^0	0.41801×10^{-1}	5	61.03
LFM	1	0.84038×10^{-1}	0.36974×10^0	0.14835×10^{-1}	348	131.77
	2	0.13191×10^0	0.54444×10^0	0.29670×10^{-1}	236	106.84
	3	0.17374×10^0	0.68508×10^0	0.44507×10^{-1}	188	96.55
MEM	1	0.12321×10^0	0.53633×10^0	0.15970×10^{-1}	5	63.55
	2	0.15423×10^0	0.61879×10^0	0.28543×10^{-1}	5	58.94
	3	0.23716×10^0	0.86819×10^0	0.41863×10^{-1}	5	57.66

various amounts of noise added into the temperature, $T|_{\Gamma_0} \equiv T|_{\Gamma_{\text{int}}}$, i.e. $p_T \in \{1\%, 2\%, 3\%\}$, for Problem II.2. Although not presented, it should be mentioned that similar results have been obtained for the Cauchy problems associated with the modified Helmholtz equation with perturbed Cauchy data given on the internal boundary, Γ_{int} , as well as the Helmholtz equation with perturbed Cauchy data given on the external boundary, Γ_{out} , i.e. Problems I.2 and II.1, respectively. From the numerical results presented in this section and illustrated in Figs. 4 and 5, it can be concluded that the stopping criterion developed in Sect. 5.4 has a regularizing effect and the numerical solution obtained by the combined MEM–BEM described in this paper is convergent and stable with respect to increasing the mesh size discretisation and decreasing the level of noise added into the input data, respectively.

5.6 Comparison with other iterative methods

It is the purpose of this section to compare the numerical results retrieved using the MEM, presented in Sect. 4.2, and its associated stopping rule given by Eq. 55, with those obtained using the other two iterative methods described in Sects. 3.3 and 4.1, i.e. the LFM and CGM, respectively, along with the stopping criterion described by Eq. 54. To do so, we set $N_{\text{int}} = N_{\text{out}}/2 = 80$ for both Problems I.2 and II.1, and also consider a fixed relative percentage level of noise added into the boundary temperature data, $T|_{\Gamma_0}$, namely $p_T = 3\%$ and $p_T = 5\%$ in the case of Problems I.2 and II.1, respectively. From the numerical experiments carried out in this study, the optimal value, τ_{opt} , for the parameter τ in the stopping rule (54) associated with the LFM and CGM was found to be $\tau_{\text{opt}} \approx 1.01$.

Figure 6a, b shows the numerical solutions for the temperature, T , and normal heat flux, ϕ , respectively, in comparison

with their corresponding analytical values, obtained using $p_T = 3\%$, the MEM and its associated stopping rule Eq. 55, and the CGM and LFM, along with the stopping criterion described by Eq. 54, for Problem I.2. For this value of p_T , the LFM, CGM and MEM are stopped after $k_{\text{opt}} = 188$, $k_{\text{opt}} = 5$ and $k_{\text{opt}} = 5$ iterations, respectively, as can be seen from Table 1 which presents the values of the optimal iteration number, k_{opt} , the corresponding accuracy errors, $e_T^a(k_{\text{opt}})$ and $e_\phi^a(k_{\text{opt}})$, the convergence error, $e_T^c(k_{\text{opt}})$ or $E_c(k_{\text{opt}})$, and the computational time, obtained using the CGM, LFM and MEM and various amounts of noise added into the boundary temperature data, i.e. $p_u \in \{1\%, 2\%, 3\%\}$, for Problem I.2. From this table, as well as Fig. 6a, b, it can be seen that in terms of accuracy, the CGM outperforms the LFM followed by the MEM for each level of noise considered in the case of Problem I.2. Although not presented here, it is reported that the same conclusion remains valid for the Problem I.1, i.e. for Cauchy problems associated with the modified Helmholtz equation. Moreover, all these iterative methods produce stable and reasonably accurate numerical solutions.

However, apart from the dependence on the parameter γ , and also as a consequence of the choice made for it (i.e. very small values for γ in order for the LFM to converge), the major disadvantage of the LFM is represented by the large number of iterations performed until the numerical solution on the under-specified boundary is obtained. Thus, especially for large-scale problems, this becomes an inconvenience with respect to the computational time required by this iterative method. For Problem I.2, the CPU times needed for the LFM, CGM and MEM to reach the numerical solutions for the temperature and normal heat flux on Γ_1 were found to be 96.55, 61.03 and 57.66 s, respectively, with the mention that all numerical computations have been performed in

FORTRAN 90 in double precision on a 3.00 GHz Intel Pentium 4 machine.

Similar results have been obtained using the three iterative methods compared in this section for Problem II.1 and these are presented in Fig. 7a, b that shows the analytical and numerical solutions for T and ϕ , respectively, with $p_T = 5\%$. Also, the values of the optimal iteration number, k_{opt} , the corresponding accuracy errors, $e_T^a(k_{opt})$ and $e_\phi^a(k_{opt})$, the convergence error, $e_T^c(k_{opt})$ or $E_c(k_{opt})$, and the computational time, obtained using the CGM, LFM and MEM and various amounts of noise added into the boundary temperature data, i.e. $p_T \in \{1\%, 2\%, 3\%, 4\%, 5\%\}$, for Problem II.1, are presented in Table 2. It is important to mention that, in terms of accuracy, the LFM outperforms the CGM followed by the MEM for each level of noise considered, in the case of both Problems II.1 and II.2, i.e. Cauchy problems associated with the Helmholtz equation. Overall, from Figs. 6 and 7, as well as Tables 1 and 2, we can conclude that stable and reasonably accurate numerical solutions are obtained by employing all iterative methods analysed in this study, with the mention that the CGM and MEM outperform the LFM as far as computational times are concerned.

6 Conclusions

In this paper, the Cauchy problem for Helmholtz-type equations with $L^2(\Gamma_0)$ boundary data was investigated numerically using yet another iterative method, namely the MEM. This rather weak requirements for the Cauchy data offer practical applicability of the proposed approach. However, the regularity of the solution is affected in this case and this represents a drawback of the present method. An associated stopping criterion, necessary for ceasing the iterations at the point where the accumulation of noise becomes dominant and the errors in predicting the exact solution increase, was also developed. On using the BEM, the iterative parameter-free MEM, which reduced the Cauchy problem to solving a sequence of well-posed, mixed, boundary value problems in $L^2(\Omega)$, was numerically implemented for two benchmark inverse problems for both the Helmholtz and modified Helmholtz equations in a two-dimensional, smooth, doubly connected domain. For all examples investigated, the numerical results obtained using various numbers of boundary elements and various amounts of noise added into the input data showed that the MEM, in conjunction with the BEM, produces a convergent and stable numerical solution with respect to increasing the number of boundary elements and decreasing the amount of noise, respectively. Although not presented in this paper, it is important to mention that a limitation of the MEM applied to solving the Cauchy problem for Helmholtz-type equations is given by the fact that especially discontinuous Neumann data on the under-spec-

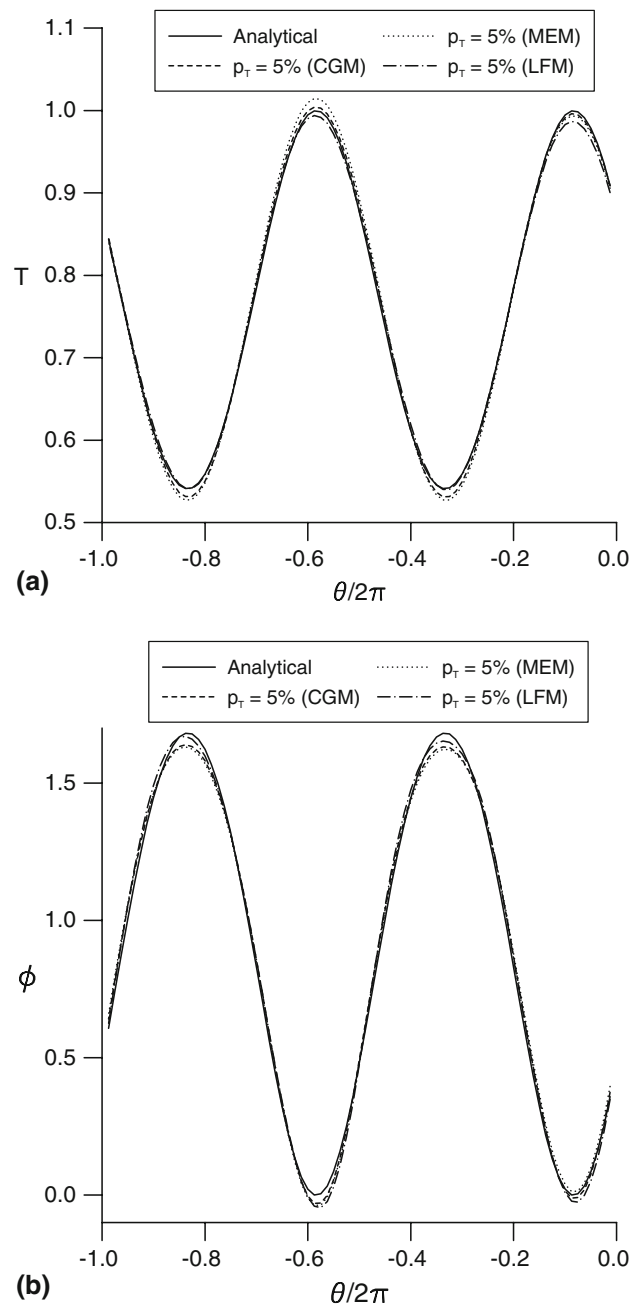


Fig. 7 The analytical (solid line) and numerical (a) temperatures T , and (b) fluxes ϕ , obtained on the under-specified boundary $\Gamma_1 \equiv \Gamma_{int}$ using $N_{out} = 160$ and $N_{int} = 80$ constant boundary elements for discretising Γ_{out} and Γ_{int} , respectively, the MEM (dotted line), CGM (dashed line) and LFM (dotted dash line), and $p_T = 5\%$ noise added into the boundary temperature, $T|_{\Gamma_0} \equiv T|_{\Gamma_{out}}$, for Problem II.1

ified boundary cannot be accurately recovered by employing the present iterative method. This result is similar to that obtained recently in the case of isotropic linear elasticity [27].

Furthermore, the MEM was also compared with another two iterative methods, more precisely with a parameter-free

Table 2 The values of the optimal iteration number, k_{opt} , the corresponding accuracy errors, $e_T^a(k_{\text{opt}})$ and $e_\phi^a(k_{\text{opt}})$, the convergence error, $e_T^c(k_{\text{opt}})$ or $E_c(k_{\text{opt}})$, and the computational time, obtained using $N_{\text{out}} = 160$ and $N_{\text{int}} = 80$ constant boundary elements for disre-

tising the outer and inner boundaries, respectively, the CGM, LFM and MEM and various relative percentage levels of noise added into the boundary temperature data, i.e. $p_T \in \{1\%, 2\%, 3\%, 4\%, 5\%\}$, for Problem II.1

Method	p_T (%)	$e_T^a(k_{\text{opt}})$	$e_\phi^a(k_{\text{opt}})$	$e_T^c(k_{\text{opt}})/E_c(k_{\text{opt}})$	k_{opt}	CPU time (s)
CGM	1	0.62567×10^{-2}	0.44710×10^{-1}	0.85904×10^{-2}	4	77.11
	2	0.70062×10^{-2}	0.45367×10^{-1}	0.16869×10^{-1}	4	76.95
	3	0.79226×10^{-2}	0.46352×10^{-1}	0.25098×10^{-1}	4	76.47
	4	0.89882×10^{-2}	0.47684×10^{-1}	0.33318×10^{-1}	4	74.14
	5	0.10178×10^{-1}	0.49370×10^{-1}	0.41544×10^{-1}	4	72.33
LFM	1	0.52898×10^{-2}	0.38915×10^{-1}	0.86503×10^{-2}	438	164.31
	2	0.62352×10^{-2}	0.42296×10^{-1}	0.17296×10^{-1}	370	154.23
	3	0.73709×10^{-2}	0.45734×10^{-1}	0.25940×10^{-1}	333	149.64
	4	0.86479×10^{-2}	0.49349×10^{-1}	0.34593×10^{-1}	307	138.70
	5	0.10010×10^{-1}	0.53094×10^{-1}	0.43250×10^{-1}	287	130.70
MEM	1	0.66040×10^{-2}	0.45425×10^{-1}	0.99334×10^{-2}	3	69.78
	2	0.84856×10^{-2}	0.47075×10^{-1}	0.18680×10^{-1}	3	69.39
	3	0.11246×10^{-1}	0.50188×10^{-1}	0.27673×10^{-1}	3	69.08
	4	0.14616×10^{-1}	0.54800×10^{-1}	0.36729×10^{-1}	3	68.98
	5	0.18473×10^{-1}	0.60875×10^{-1}	0.45807×10^{-1}	3	67.97

procedure (CGM), as well as a parameter-dependent method (LFM), together with their associated regularizing stopping criteria, which were previously introduced by Marin et al. [32,34], respectively. It was shown that, in terms of accuracy, the CGM outperforms the LFM and the latter outperforms the MEM for Cauchy problems associated with the modified Helmholtz equation. In the case of similar inverse problems for the Helmholtz equation, the LFM provides us with the best numerical results in terms of accuracy, followed by the CGM, whilst the MEM is outperformed by the CGM. The LFM requires the choice of the parameter γ in a suitable range in order to achieve the convergence of this numerical method. This is achieved by choosing a sufficiently small value for the parameter γ (in practice, $\gamma \approx 0.1$), which implies a much larger number of iterations until the numerical solution is obtained than those required by the parameter-free methods analysed in this paper. Consequently, especially for large-scale problems, the CGM and MEM are preferred to the LFM since the latter is quite slow in comparison with the aforementioned parameter-free methods as far as CPU times are concerned. To conclude, in terms of convergence rate, stability and accuracy, among the iterative methods analysed in this paper, the parameter-free methods MEM and CGM are recommended to be used, with a special mention for the latter. Future work will be related to the application of the MEM to solving numerically the Cauchy problem associated with Helmholtz-type operators in domains with corners.

References

1. Bastay G, Kozlov VA, Turesson B (2001) Iterative methods for and inverse heat conduction problem. *J Inverse Ill-Posed Prob* 9: 375–388
2. Beskos DE (1997) Boundary element method in dynamic analysis, Part II (1986–1996). *ASME Appl Mech Rev* 50:149–197
3. Chen G, Zhou J (1992) Boundary element methods. Academic Press, London
4. Chen JT, Wong FC (1998) Dual formulation of multiple reciprocity method for the acoustic mode of a cavity with a thin partition. *J Sound Vib* 217:75–95
5. DeLillo T, Isakov V, Valdivia N, Wang L (2001) The detection of the source of acoustical noise in two dimensions. *SIAM J Appl Math* 61:2104–2121
6. DeLillo T, Isakov V, Valdivia N, Wang L (2003) The detection of surface vibrations from interior acoustical pressure. *Inverse Probl* 19:507–524
7. Engl HW, Hanke M, Neubauer A (1996) Regularization of inverse problems. Kluwer, Boston
8. Hadamard J (1923) Lectures on Cauchy problem in linear partial differential equations. Oxford University Press, London
9. Hall WS, Mao XQ (1995) A boundary element investigation of irregular frequencies in electromagnetic scattering. *Eng Anal Bound Elem* 16:245–252
10. Hanke M (1995) Conjugate gradient type methods for ill-posed problems. Longman Scientific and Technical, New York
11. Hanke M (1995) The minimal error conjugate gradient method is a regularization method. *Proc Am Math Soc* 123:3487–3497
12. Hào DN, Reinhardt H-J (1998) Gradient methods for inverse heat conduction problems. *Inverse Probl Eng* 6:177–211
13. Hào DN, Lesnic D (2000) The Cauchy problem for Laplace's equation via the conjugate gradient method. *IMA J Appl Math* 65: 199–217

14. Harari I, Barbone PE, Slavutin M, Shalom R (1998) Boundary infinite elements for the Helmholtz equation in exterior domains. *Int J Numer Methods Eng* 41:1105–1131
15. Jin B, Marin L (2008) The plane wave method for inverse problems associated with Helmholtz-type equations. *Eng Anal Bound Elem* 32:223–240
16. Jin B, Zheng Y (2005) Boundary knot method for some inverse problems associated with the Helmholtz equation. *Int J Numer Methods Eng* 62:1636–1651
17. Jin B, Zheng Y (2005) Boundary knot method for the Cauchy problem associated with the inhomogeneous Helmholtz equation. *Eng Anal Bound Elem* 29:925–935
18. Jin B, Zheng Y (2006) A meshless method for some inverse problems associated with the Helmholtz equation. *Comput Methods Appl Mech Eng* 195:2270–2288
19. Johansson T (2000) Reconstruction of a Stationary Flow from Boundary Data. Dissertations No. 853, Linköping Studies in Science and Technology
20. Johansson T, Lesnic D (2006) A variational conjugate gradient method for determining the fluid velocity of a slow viscous flow. *Appl Anal* 85:1327–1341
21. Johansson T, Lesnic D (2006) Reconstruction of a stationary flow from incomplete boundary data using iterative methods. *Eur J Appl Math* 17:651–663
22. Johansson T, Lesnic D (2007) An iterative method for the reconstruction of a stationary flow. *Numer Methods Partial Differ Equ* 23:998–1017
23. King JT (1989) The minimal error conjugate gradient method for ill-posed problems. *J Optim Theory Appl* 60:297–304
24. Kraus AD, Aziz A, Welty J (2001) *Extended surface heat transfer*. Wiley, New York
25. Landweber L (1951) An iteration formula for Fredholm integral equations of the first kind. *Am J Math* 73:615–624
26. Marin L (2005) A meshless method for the numerical solution of Cauchy problem associated with three-dimensional Helmholtz-type equations. *Appl Math Comput* 165:355–374
27. Marin L (2009) The minimal error method for the Cauchy problem in linear elasticity. Numerical implementation for two-dimensional homogeneous isotropic linear elasticity. *Int J Solids Struct* 46:957–974
28. Marin L, Lesnic D (2005) The method of fundamental solutions for the Cauchy problem associated with two-dimensional Helmholtz-type equations. *Comput Struct* 83:267–278
29. Marin L, Lesnic D (2005) Boundary element—Landweber method for the Cauchy problem in linear elasticity. *IMA J Appl Math* 18:817–825
30. Marin L, Hào DN, Lesnic D (2002) Conjugate gradient-boundary element method for the Cauchy problem in elasticity. *Quart J Mech Appl Math* 55:227–247
31. Marin L, Elliott L, Heggs PJ, Ingham DB, Lesnic D, Wen X (2003) An alternating iterative algorithm for the Cauchy problem associated to the Helmholtz equation. *Comput Methods Appl Mech Eng* 192:709–722
32. Marin L, Elliott L, Heggs PJ, Ingham DB, Lesnic D, Wen X (2003) Conjugate gradient-boundary element solution to the Cauchy problem for Helmholtz-type equations. *Comput Mech* 31:367–377
33. Marin L, Elliott L, Heggs PJ, Ingham DB, Lesnic D, Wen X (2004) Comparison of regularization methods for solving the Cauchy problem associated with the Helmholtz equation. *Int J Numer Methods Eng* 60:1933–1947
34. Marin L, Elliott L, Heggs PJ, Ingham DB, Lesnic D, Wen X (2004) BEM solution for the Cauchy problem associated with Helmholtz-type equations by the Landweber method. *Eng Anal Bound Elem* 28:1025–1034
35. Marin L, Elliott L, Heggs PJ, Ingham DB, Lesnic D, Wen X (2006) Dual reciprocity boundary element method solution of the Cauchy problem for Helmholtz-type equations with variable coefficients. *J Sound Vib* 297:89–105
36. Morozov VA (1966) On the solution of functional equations by the method of regularization. *Soviet Math Doklady* 167:414–417
37. Nemirovskii AS (1986) Regularizing properties of the conjugate gradient method in ill-posed problems. *USSR Comput Math Math Phys* 26:7–16
38. Qin HH, Wen DW (2009) Tikhonov type regularization method for the Cauchy problem of the modified Helmholtz equation. *Appl Math Comput* (in press)
39. Qin HH, Wei T, Shi R (2009) Modified Tikhonov regularization method for the Cauchy problem of the Helmholtz equation. *J Comput Appl Math* 224:39–53
40. Tumakov DN (2006) The Cauchy problem for the Helmholtz equation in a domain with a piecewise-smooth boundary. *Mathematical Methods in Electromagnetic Theory, MMET, Conference Proceedings*, art. no. 1689818, pp. 446–448
41. Wei T, Qin HH, Shi R (2008) Numerical solution of an inverse 2D Cauchy problem connected with the Helmholtz equation. *Inverse Problems*, vol 24, art. no. 035003
42. Xiong X-T, Fu C-L (2007) Two approximate methods of a Cauchy problem for the Helmholtz equation. *Comput Appl Math* 26:285–307